

# TAL1 cooperates with PI3K/AKT pathway activation in T-cell acute lymphoblastic leukemia

Naomi Thielemans,<sup>1,2,3</sup> Sofie Demeyer,<sup>1,2,3</sup> Nicole Mentens,<sup>1,2,3</sup> Olga Gielen,<sup>1,2,3</sup> Sarah Provost<sup>1,2,3</sup> and Jan Cools<sup>1,2,3</sup>

<sup>1</sup>Center for Human Genetics, KU Leuven; <sup>2</sup>Center for Cancer Biology, VIB and <sup>3</sup>Leuven Cancer Institute (LKI), KU Leuven – UZ Leuven, Leuven, Belgium

**Correspondence:** J. Cools  
[jan.cools@kuleuven.be](mailto:jan.cools@kuleuven.be)

**Received:** July 28, 2021.  
**Accepted:** March 22, 2022.  
**Prepublished:** March 31, 2022.

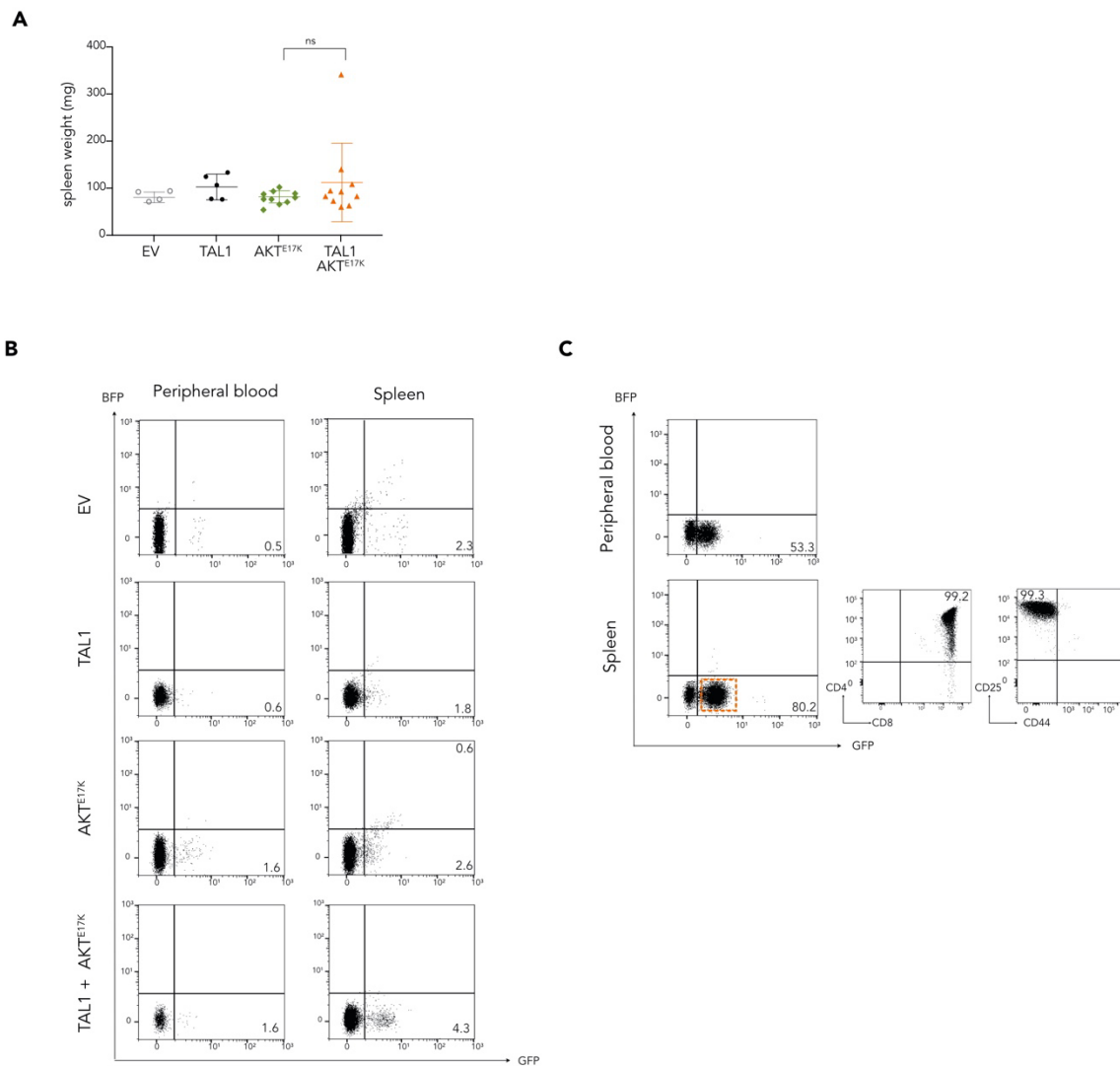
<https://doi.org/10.3324/haematol.2021.279718>

©2022 Ferrata Storti Foundation  
Published under a CC BY-NC license 

## TAL1 cooperates with PI3K/AKT pathway activation in T-cell acute lymphoblastic leukemia

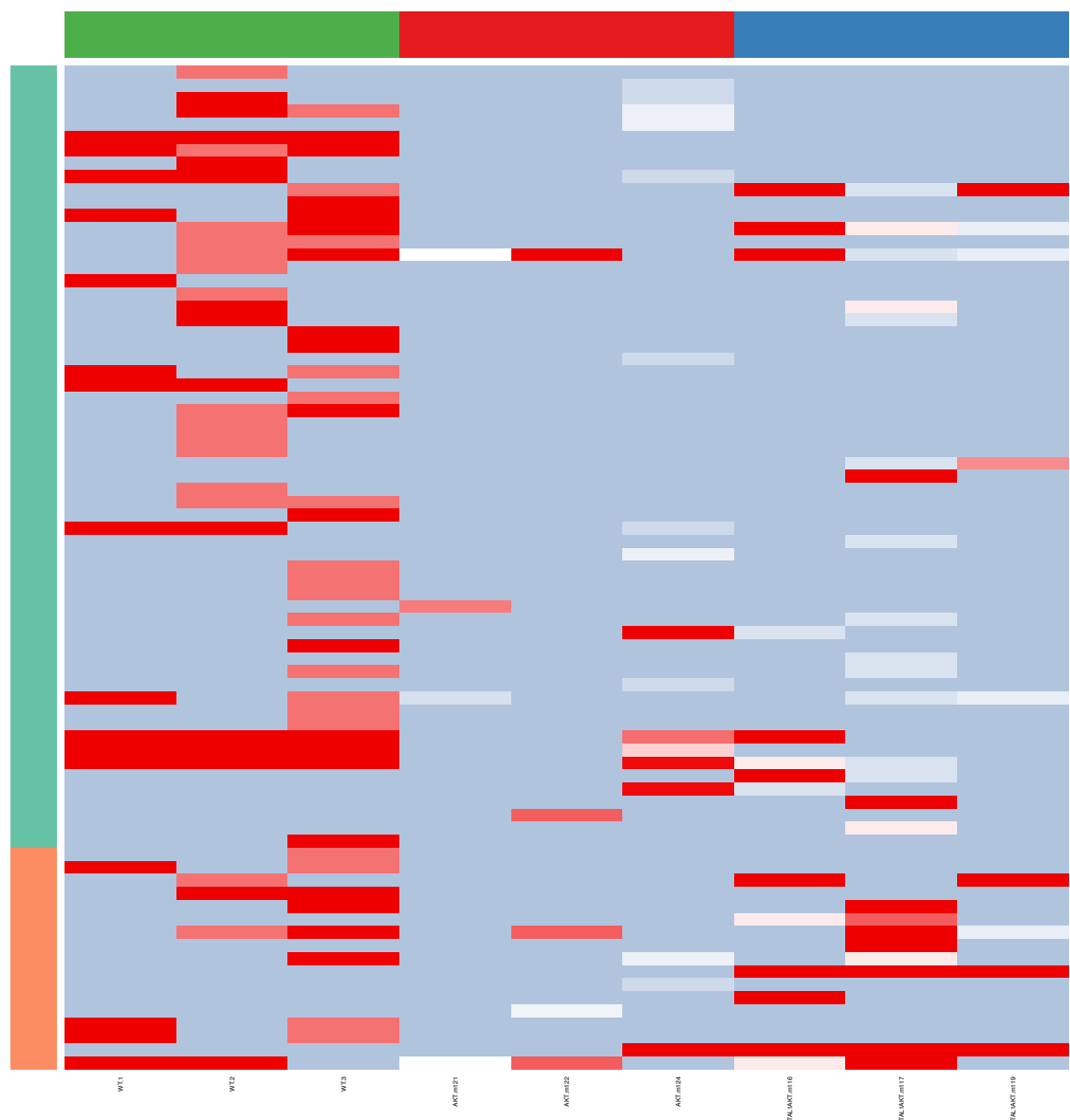
Naomi Thielemans, Sofie Demeyer, Nicole Mentens, Olga Gielen, Sarah Provost, Jan Cools

### Supplementary Figures



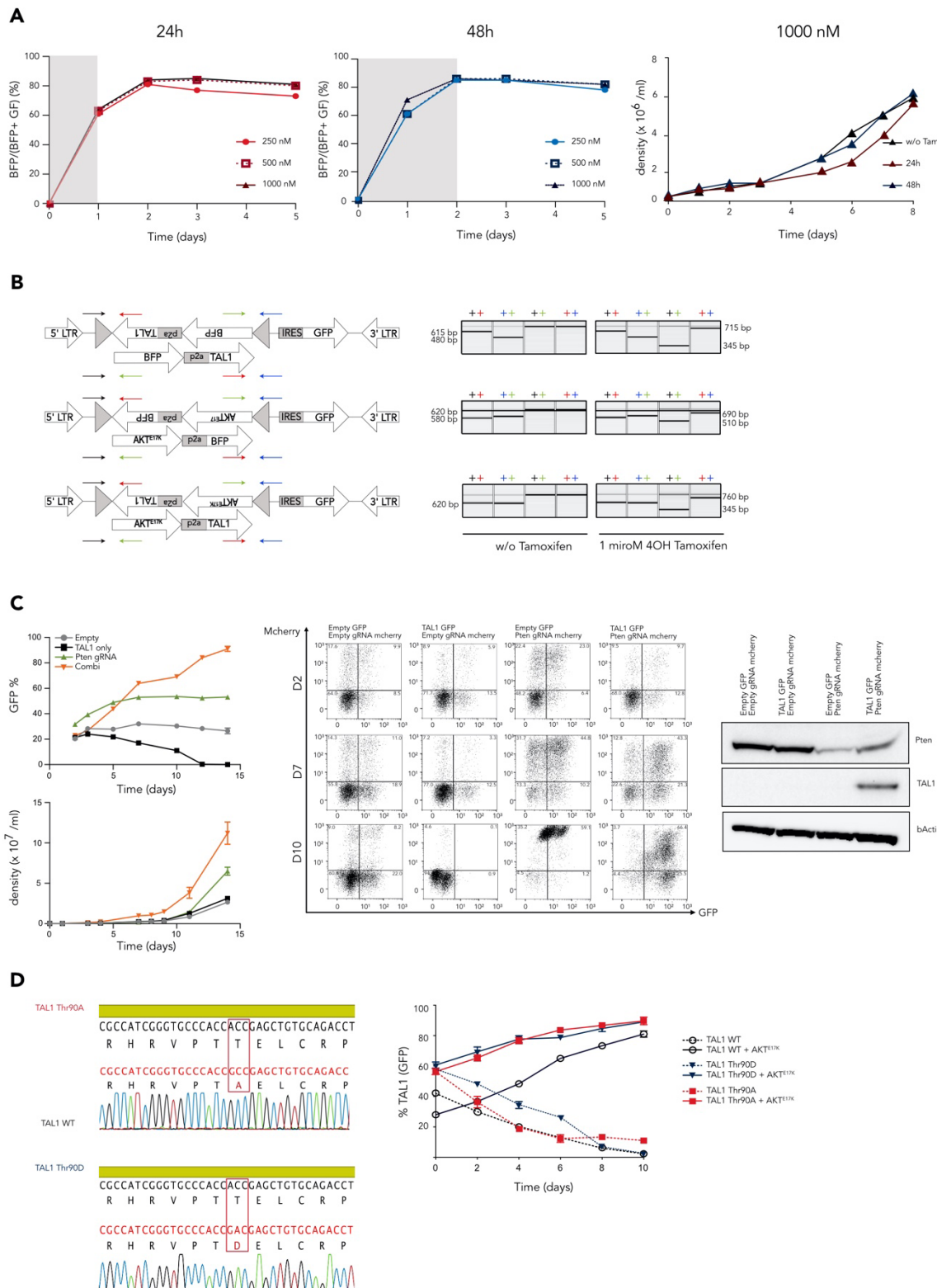
### Supplementary Figure 1.

**A**, Plot showing spleen weight at time of sacrifice. P-values were calculated using the one-way ANOVA with Tukey correction to account for multiple comparisons. **B**, Flow cytometry analysis of peripheral blood and spleen at time of sacrifice- BFP y-axis; GFP x-axis. **C**, Flow cytometry analysis of peripheral blood and spleen of secondary transplant mouse. Spleen cells were ) were stained for CD8 (APC-eFluor 780, X-axis) and CD4 (PE-Cy7, Y axis) and stained for CD25 (APC, X-axis) and CD44 (PerCP-Cy5.,5 Y-axis).



### Supplementary Figure 2. Clonality of mouse lymphoma/leukemia.

RNA-seq data from RNA extracted from thymus cells in wild type mice ( $n=3$ , left), AKT(E17K) ( $n=3$ , middle) or TAL1+AKT(E17K) ( $n=3$ , right) lymphoma/leukemia cells (primary disease) was analyzed for the expression of the various variable regions for T-cell receptor alpha or beta. Upon rearrangement of the T-cell receptors, only one variable region is selected and expressed and therefore expression data provides an estimate of the various clones present in thymus. The pattern observed in AKT(E17K) or TAL1+AKT(E17K) mice corresponds to an oligoclonal origin of the disease.



**Supplementary Figure 3.**

**A**, Treatment of Cre-ER cells with empty vector: percentage of floxed cells (= BFP/(BFP+GFP)) over time. Cells were treated with different doses of 4-OH-Tamoxifen (250-500-100 nM). Cells were treated during 24h (left) or during 48h (middle). Right: effect on cell viability after treatment with 1000 nM 4OH-Tamoxifen for different hours. **B**, Schematic overview of different inducible constructs. Colored arrows indicate different primers (left). Results of PCR with indicated primers after DNA extraction of pro-T cells showing successful flipping of the construct on DNA level. (right). **C**, Pro-T cells derived from a CAS9 donor mice and transduced with different constructs. Left: growth curves showing GFP% (= TAL1 or empty vector) over time and cell density (mean with SD) over time, both showing that TAL1-Pten<sup>del</sup> combination rescues TAL1 cell growth. Middle: Flow cytometry analysis of pro-T cells at different time points. Right: Western blotting, confirming expression of TAL1 in TAL1-Pten<sup>del</sup> transformed pro-T cells and confirming deletion of Pten in Pten<sup>del</sup> and TAL1-Pten<sup>del</sup> cells. **D**, Results of sanger sequencing after PCR-mutagenesis of TAL1 showing point mutations at Thr90. Threonine was either replaced by an alanine (above) or an aspartic acid (below). Right: % of GFP = (TAL1) over time of different TAL1 variants (WT, Thr90A, Thr90D).

(next page)

**Supplementary Figure 4. Heatmaps of deregulated genes in pro-T cells or mouse models.**

Figure shows selected heatmaps of comparisons between various conditions in pro-T cells or mouse lymphoma/leukemia models. Genes are indicated in rows, samples in columns.

Additional data on deregulated gene expression based on RNA-seq data is provided in supplementary excel tables.

